NASA TECHNICAL NOTE

NASA TN D-2675

NASA TN D-2675

A TENSION SHELL STRUCTURE FOR APPLICATION TO ENTRY VEHICLES

by Melvin S. Anderson, James C. Robinson, Harold G. Bush, and Robert W. Fralich

Langley Research Center
Langley Station, Hampton, Va.

NATIONAL AERONAUTICS AND SPACE ADMINISTRATION • WASHINGTON, D. C. • MARCH 1965

A TENSION SHELL STRUCTURE FOR APPLICATION TO ENTRY VEHICLES

By Melvin S. Anderson, James C. Robinson,
Harold G. Bush, and Robert W. Fralich

Langley Research Center
Langley Station, Hampton, Va.

NATIONAL AERONAUTICS AND SPACE ADMINISTRATION

For sale by the Office of Technical Services, Department of Commerce,
Washington, D.C. 20230 -- Price $1.00

A TENSION SHELL STRUCTURE FOR APPLICATION TO ENTRY VEHICLES

By Melvin S. Anderson, James C. Robinson,
Harold G. Bush, and Robert W. Fralich
Langley Research Center

SUMMARY

The shape of a shell of revolution designed to have only tensile stresses under axisymmetric aerodynamic loadings has been derived on the basis of linear membrane theory. The drag coefficient for various proportions and various values of circumferential tension is also given. The results of this paper indicate that the design of an entry vehicle based on the tension shell concept leads to desirable aerodynamic and structural characteristics, namely, high drag and low weight.

INTRODUCTION

The discussion of entry into thin planetary atmospheres presented in references 1 and 2 indicates that for such an environment, a very low value of the ballistic coefficient would be necessary to obtain reasonable dwell times in the atmosphere or to obtain low enough speeds for parachute deployment. As the ballistic coefficient decreases, the structural weight fraction increases, and for thin atmospheres such as that of Mars the structural weight can become so large that conventional structural concepts lead to a vehicle with little payload capability. This behavior is due in part to the fact that the structural design of most aircraft and entry vehicles is controlled by loading conditions that cause buckling to be a primary design factor. Thus, stresses are lower than the material strength capability. In order to take better advantage of the strength of the material, a structural concept has been developed which resists the primary structural loadings by tensile stresses over a major portion of the vehicle surface and thus permits a more efficient structural design. This concept, shown in figure 1(a), was introduced in reference 1 as a possible solution to the problem of entry into thin planetary atmospheres. The payload is assumed to be concentrated in the forward portion of the vehicle and supported by a shell that is shaped to resist the aerodynamic loadings by tensile stresses. The tension in the shell is resisted by a compression ring at the base of the vehicle. The purpose of this paper is to describe the mathematical development of the tension shell concept and to discuss some of its characteristics.

SYMBOLS

a_1, a_2, a, a' constants of integration

A^2 shape parameter associated with Newtonian pressure, $\frac{Kqr_b}{2N_o}$

B^2 shape parameter associated with uniform pressure, $\frac{p_o r_b}{2N_o}$

C^2 shape parameter in equation (34) defining proportion of catenary curve

C_D drag coefficient, $\frac{D}{q\pi r_b^2}$

D drag force

$\operatorname{erf}(A) = \frac{2}{\sqrt{\pi}} \int_0^A e^{-x^2} dx$ error function

$E(\epsilon,\delta) = \int_0^\epsilon \sqrt{1 - \delta^2 \sin^2 x}\, dx$ elliptic integral of second kind

$F(\epsilon,\delta) = \int_0^\epsilon \frac{dx}{\sqrt{1 - \delta^2 \sin^2 x}}$ elliptic integral of first kind

$G = \frac{2B^2}{1 + \sqrt{1 + 4B^4}}$

$I_n(\lambda), K_n(\lambda)$ modified Bessel functions of order n

k integer

K constant used in Newtonian pressure distribution

n order of Bessel function

N_θ, N_φ circumferential and meridional stress resultants, respectively, positive in tension

N_o N_φ evaluated at $r = r_b$

p pressure acting on shell, positive outward

p_o magnitude of uniform external pressure

q dynamic pressure of airstream

r radial coordinate

r_a, r_b radius of tension shell at forward end and at base, respectively

r_1, r_2 principal radii of curvature of shell in meridional and circumferential directions, respectively

u new dependent variable in differential equation (see eq. (11))

z longitudinal coordinate of shell

$$\alpha = \frac{N_\theta}{N_\varphi}$$

$$\beta = \sqrt{1 - G^4}$$

$$\gamma = \sin^{-1}\sqrt{\frac{1 + B^2(1 - \rho^2)}{2}}$$

$$\Gamma(n) = \int_0^\infty e^{-x} x^{n-1} dx \qquad \text{gamma function}$$

$$\delta = \sqrt{\frac{1 + B^2}{2}}$$

$$\epsilon = \cos^{-1}\rho\sqrt{\frac{B^2}{1 + B^2}}$$

$$\epsilon_1 = \cos^{-1}\sqrt{\frac{B^2}{1 + B^2}}$$

$$\eta = \sin^{-1}\sqrt{\frac{1 - G^2\rho^2}{1 - G^4}}$$

$$\eta_1 = \sin^{-1}\sqrt{\frac{1}{1 + G^2}}$$

θ circumferential coordinate

$$\lambda = \frac{2A^2\rho^{2-\alpha}}{2 - \alpha}$$

$$\lambda_1 = \frac{2A^2}{2 - \alpha}$$

$\rho = \frac{r}{r_b}$ nondimensional radial coordinate

ρ_∞ value of ρ for which $\tan \varphi$ is infinite

$\rho_a = \frac{r_a}{r_b}$

φ meridional coordinate

$$\psi(A) = \int_0^A e^{x^2} dx$$

MATHEMATICAL DEVELOPMENT OF THE SHAPE OF THE TENSION SHELL STRUCTURE

In the mathematical development of the shape of the tension shell structure presented herein, an axisymmetric vehicle is considered to be entering a low-density atmosphere. It is improbable that the structural shell of such a vehicle can be designed so that tensile stresses exist for all loading conditions. However, a design can be made such that at zero angle of attack sufficient tension can be provided to allow for deviations from this condition. The mathematical development of this configuration is based on the following assumptions: (1) The structure is a shell of revolution subject to an axisymmetric pressure distribution. (See fig. 1 for configuration and coordinate system.) (2) The pressure loading is assumed to produce a pure membrane state of stress based on linear membrane theory with N_θ/N_φ some constant ratio. (3) The aft end of the shell terminates with a compression ring. (See fig. 1(a).) Although the design of the ring is not considered in this analysis, the concentration of the compression material in a single member would be expected to lead to an efficient design. (4) The dimensions of the shell are large compared with the dimensions of the payload, which is assumed to be concentrated at the small forward end and supported by a ring. This assumption is reasonable for lightly loaded vehicles entering low-density atmospheres.

The analysis proceeds from the appropriate membrane equilibrium equations for a shell of revolution subject to axisymmetric loadings. These equations are (see ref. 3)

$$\frac{d(rN_\varphi)}{d\varphi} - r_1 N_\theta \cos \varphi = 0 \tag{1}$$

$$\frac{N_\varphi}{r_1} + \frac{N_\theta}{r_2} = p \tag{2}$$

where

$$\frac{1}{r_1} = \cos \varphi \frac{d\varphi}{dr} = \frac{d \sin \varphi}{dr} \tag{3}$$

$$\frac{1}{r_2} = \frac{\sin \varphi}{r} \tag{4}$$

It is assumed that there is no force in the z-direction on the compression ring at $r = r_b$. Therefore, the curve of the meridian must have a horizontal tangent at $r = r_b$; thus,

$$\frac{dz}{dr} = -\tan \varphi = 0 \tag{5}$$

If $N_\theta = \alpha N_\varphi$ where α is a constant, equation (1) becomes

$$\frac{dN_\varphi}{dr} + \frac{1 - \alpha}{r} N_\varphi = 0 \tag{6}$$

The solution for N_φ is

$$r^{(1-\alpha)} N_\varphi = \text{Constant} = N_o r_b^{(1-\alpha)} \tag{7}$$

It should be noted that this solution is independent of the pressure distribution and that for the case $\alpha = 1$, N_φ is constant throughout the shell. (From the definition of α, N_θ also has the same constant value.) With the use of equations (3), (4), and (7), equation (2) becomes

$$\frac{d \sin \varphi}{dr} + \frac{\alpha}{r} \sin \varphi - \frac{p}{N_o}\left(\frac{r}{r_b}\right)^{1-\alpha} = 0 \tag{8}$$

This equation may be solved for $\sin \varphi$ for any pressure distribution; then, $\tan \varphi$, which equals $-dz/dr$, is determined, and if this is integrated with respect to r, the z-coordinates of the desired configuration are obtained as a function of r. Solutions have been obtained for two pressure distributions, that given by Newtonian impact theory and that resulting from a uniform pressure distribution. These solutions are presented in the following sections.

Newtonian Pressure Distribution

The pressure given by Newtonian theory is taken in the form

$$p = -Kq \cos^2\varphi \tag{9}$$

By substituting equation (9) into equation (8) and by using $\rho = r/r_b$, the differential equation for $\sin\varphi$ becomes

$$\frac{d \sin\varphi}{d\rho} + \frac{\alpha}{\rho} \sin\varphi + 2A^2\rho^{(1-\alpha)}\left(1 - \sin^2\varphi\right) = 0 \tag{10}$$

where

$$A^2 = \frac{Kqr_b}{2N_o}$$

This nonlinear differential equation is a form of the Riccati equation and may be solved by using the following substitution (see ref. 4):

$$\sin\varphi = -\frac{du}{d\rho} \frac{1}{2A^2u\rho^{(1-\alpha)}} \tag{11}$$

Equation (10) then becomes

$$\frac{d^2u}{d\rho^2} - \frac{1 - 2\alpha}{\rho} \frac{du}{d\rho} - 4A^4u\rho^{(2-2\alpha)} = 0 \tag{12}$$

The solution for u if $\frac{1 - \alpha}{2 - \alpha}$ does not equal an integer is

$$u = \rho^{(1-\alpha)}\left[a_1I_n(\lambda) + a_2I_{-n}(\lambda)\right] \tag{13}$$

where

$$n = \frac{1 - \alpha}{2 - \alpha} \tag{14}$$

$$\lambda = \frac{2A^2\rho^{(2-\alpha)}}{2 - \alpha} \tag{15}$$

and I_n is the modified Bessel function of the first kind of order n. Substituting equation (13) into equation (11) (see ref. 5 for properties of Bessel functions and their derivatives) gives

$$\sin \varphi = - \frac{I_{n-1}(\lambda) + aI_{1-n}(\lambda)}{I_n(\lambda) + aI_{-n}(\lambda)} \tag{16}$$

where

$$a = \frac{a_2}{a_1}$$

From equation (14) it can be seen that as α varies from 0 to 1, n varies from 1/2 to 0 and, therefore, equation (16) will generally involve the fractional-order Bessel functions. The boundary condition, given as equation (5), implies that $\sin \varphi = 0$ at $\rho = 1$. Therefore,

$$a = - \frac{I_{n-1}(\lambda_1)}{I_{1-n}(\lambda_1)} \tag{17}$$

For the special case $\alpha = 0$, $n = 1/2$; therefore, the Bessel functions appearing in equation (16) can be expressed in terms of hyperbolic functions as

$$\left.\begin{aligned} I_{1/2}(\lambda) &= \sqrt{\frac{2}{\pi\lambda}} \sinh \lambda \\ I_{-1/2}(\lambda) &= \sqrt{\frac{2}{\pi\lambda}} \cosh \lambda \end{aligned}\right\} \tag{18}$$

The expression for $\sin \varphi$ now becomes

$$\sin \varphi = \tanh A^2(1 - \rho^2) \tag{19}$$

In addition,

$$\frac{dz}{dr} = -\tan \varphi = -\sinh A^2(1 - \rho^2) \tag{20}$$

This equation can be integrated in terms of the error integral and related functions, which are tabulated in reference 5. The expression for z for $\alpha = 0$ is

$$\frac{z}{r_b} = \frac{e^{A^2}}{A} \frac{\sqrt{\pi}}{4} \left[\operatorname{erf}(A) - \operatorname{erf}(A\rho)\right] - \frac{e^{-A^2}}{2A} \left[\psi(A) - \psi(A\rho)\right] \tag{21}$$

Since in the general case negative fractional orders of the Bessel functions are involved in equation (16), which are not usually found in mathematical tables, it may be necessary to use the function

$$\frac{2}{\pi} K_n(\lambda) = \frac{1}{\sin n\pi}\left[I_{-n}(\lambda) - I_n(\lambda)\right]$$

which has been tabulated for certain fractional values of n. The expression for $\sin \varphi$ then becomes

$$\sin \varphi = \frac{K_{n-1}(\lambda) - a' I_{n-1}(\lambda)}{K_n(\lambda) + a' I_n(\lambda)} = \frac{\left(1 - a' \frac{2}{\pi} \sin n\pi\right) K_{1-n}(\lambda) - a' I_{1-n}(\lambda)}{K_n(\lambda) + a' I_n(\lambda)} \tag{22}$$

where

$$a' = \frac{K_{1-n}(\lambda_1)}{\frac{2}{\pi} \sin n\pi \, K_{1-n}(\lambda_1) + I_{1-n}(\lambda_1)} \tag{23}$$

Equation (22) is also valid for integral values of n ($\alpha = 1$, for example). In reference 5 the functions I_n and K_n are tabulated for $n = 1/3$ and $n = 2/3$, which are the functions required for $\alpha = 1/2$.

Tabulations of I_n and K_n for other fractional values of n appear to be rare and perhaps nonexistent. Hence, in the general case it is necessary to use the following series expansion for $I_n(\lambda)$ (see ref. 5):

$$I_n(\lambda) = \left(\frac{\lambda}{2}\right)^n \sum_{k=0}^{\infty} \frac{\left(\frac{\lambda}{2}\right)^{2k}}{k!\Gamma(n + k + 1)} \tag{24}$$

Once $\sin \varphi$ is determined, the z-coordinate can be obtained by a simple numerical integration of $dz/dr = -\tan \varphi$.

Since this configuration is considered for an entry vehicle, the drag coefficient is an important quantity to be determined. The drag acting on the surface of the shell lying between $r = r_a$ and $r = r_b$ may be determined simply by taking the z-component of N_φ at $r = r_a$ and integrating around the circumference. Thus,

$$D = \left(2\pi r N_\varphi \sin \varphi\right)_{r=r_a} \tag{25}$$

The drag coefficient related to the base area can be obtained for Newtonian flow from equation (7) and equation (25) as

$$C_D = \frac{D}{q\pi r_b^2} = \left(\frac{K}{A^2} \rho^\alpha \sin \varphi\right)_{r=r_a} \tag{26}$$

where $\sin \varphi$ is obtained from equation (16) or equation (22). For the special case $\alpha = 0$,

$$C_D = \frac{K}{A^2} \tanh A^2\left(1 - \rho_a{}^2\right) \tag{27}$$

Uniform Pressure Distribution

An insight into the influence of loading on the shape of the tension shell can be obtained by looking at the results for a uniformly distributed pressure, which is a significantly different loading from that applied by Newtonian flow. This uniform pressure shape can be obtained from equation (8) by setting the pressure constant ($p = -p_o$). The solution for $\sin \varphi$ then becomes

$$\sin \varphi = B^2\left[\frac{1}{\rho^\alpha} - \rho^{(2-\alpha)}\right] \tag{28}$$

where

$$B^2 = \frac{p_o r_b}{2N_o}$$

and use has been made of the boundary condition (see eq. (5)) at $r = r_b$.

For certain values of α, the z-coordinate can be expressed in terms of elliptic integrals. For example, if $\alpha = 0$

$$\frac{z}{r_b} = \frac{1}{\sqrt{2}B}\left[F(\epsilon,\delta) - F(\epsilon_1,\delta) - 2E(\epsilon,\delta) + 2E(\epsilon_1,\delta)\right] \tag{29}$$

for $B^2 \leqq 1$ and

$$\frac{z}{r_b} = \left[F\left(\gamma,\frac{1}{\delta}\right) - F\left(\frac{\pi}{4},\frac{1}{\delta}\right)\right]\cos \epsilon_1 - \left[E\left(\gamma,\frac{1}{\delta}\right) - E\left(\frac{\pi}{4},\frac{1}{\delta}\right)\right]\frac{1}{\cos \epsilon_1} \tag{30}$$

for $B^2 \geqq 1$, where

$$\delta = \sqrt{\frac{1 + B^2}{2}} \qquad \epsilon_1 = \cos^{-1}\sqrt{\frac{B^2}{1 + B^2}}$$

$$\epsilon = \cos^{-1}\rho\sqrt{\frac{B^2}{1 + B^2}} \qquad \gamma = \sin^{-1}\sqrt{\frac{1 + B^2\left(1 - \rho^2\right)}{2}}$$

and F and E are elliptic integrals of the first and second kind, respectively. For $\alpha = 1$

$$\frac{z}{r_b} = G\left[F(\eta,\beta) - F(\eta_1,\beta)\right] - \frac{1}{G}\left[E(\eta,\beta) - E(\eta_1,\beta)\right] \tag{31}$$

where

$$G = \frac{2B^2}{1 + \sqrt{1 + 4B^4}} \qquad \eta = \sin^{-1}\sqrt{\frac{1 - G^2\rho^2}{1 - G^4}}$$

$$\beta = \sqrt{1 - G^4} \qquad \eta_1 = \sin^{-1}\sqrt{\frac{1}{1 + G^2}}$$

For the general case, $\sin\varphi$ can be determined from equation (28) and z can be obtained numerically as in the case of Newtonian flow.

RESULTS AND DISCUSSION

Newtonian Flow Shape

Meridian curves have been calculated from the Newtonian flow analysis for several values of the parameters A^2 and N_θ/N_φ. The coordinates are given in table 1 and a typical set of curves is shown in figure 2. Calculations were made with a digital computer by using equation (16) for $\sin\varphi$ and the series expansion for the Bessel function (eq. (24)). Four to six terms in the series were usually found to be sufficient for the range of arguments considered. Values of $\sin\varphi$ and dz/dr were calculated for values of r/r_b at intervals of 0.01, and z was determined by a simple numerical integration. For $\alpha = 0$, the results of the numerical procedure were compared with those of the closed-form solution (see eq. (21)) and the differences were less than 0.05 percent.

Figure 2(a) shows that for $N_\theta/N_\varphi = 0$, all curves intersect the $r = 0$ axis; however, figure 2(b) shows that for $N_\theta/N_\varphi > 0$, the curves terminate at some nonzero value of r with a vertical tangent ($\sin\varphi = 1$), and some form of closure would have to be provided. Even for $N_\theta/N_\varphi = 0$, practical considerations would probably dictate terminating the tension shell at some nonzero value of r and using a compression structure such as a spherical cap for the remainder of the vehicle.

Since the drag coefficient is a very important factor in the design of an entry vehicle, it is of interest to calculate the drag coefficient for some of the more promising configurations. Accordingly, the drag coefficient is plotted in figure 3 for representative values of A^2 and N_θ/N_φ. For these

calculations, the constant K in the expression for Newtonian pressure was taken as 2. For $N_\theta/N_\varphi = 0$ the bodies were considered to terminate at a point so that C_D is given by (see eq. (27))

$$C_D = \frac{2}{A^2} \tanh A^2 \tag{32}$$

When $N_\theta/N_\varphi > 0$ the bodies were considered to have a hemispherical cap attached at the point where the tangent to the meridian curve was infinite. If this point is denoted as ρ_∞, and since the drag coefficient for a hemisphere is 1, the drag coefficient for the complete configuration is given by (see eq. (26))

$$C_D = \frac{2}{A^2} \rho_\infty{}^\alpha + \rho_\infty{}^2 \tag{33}$$

If any of these configurations were terminated at a larger radius with a segment of a spherical cap, a higher theoretical drag than that shown in figure 3 would result. Figure 3 shows that high drag coefficients can be obtained for configurations with reasonable overall proportions. Thus, the concept of the tension shell appears applicable to the design of an efficient entry vehicle. However, it should be recognized that the complete shell would not be in tension, since a payload attachment ring is required near the forward end. This ring could probably be located at $r/r_b = 1/4$ or less so the area of compressive structure compared with the total area would be quite small and would not lead to a large weight penalty. The high drag coefficients indicate that this concept might also be used to advantage for a deployable decelerator. Such a concept was proposed in reference 6 where the equation for a uniform pressure shape was given.

It should be noted that the shape is not a function of the magnitude of the loading; that is, the same configuration would be applicable throughout the range of dynamic pressures encountered in flight though, of course, the stresses would vary with dynamic pressure. Also, the shape has been derived by use of a rather simple aerodynamic theory; but use of more refined theories is probably not warranted, since other loading conditions must be considered. Deviations in flow conditions and angle of attack from that considered will change the stress situation somewhat but probably not enough to alter the basic concept of treating the shell as a tension structure.

Uniform Pressure Shape

As mentioned previously, the results for uniform pressure can be used to obtain an indication of how sensitive the shape of the tension shell is to a change in pressure distributions. Coordinates for the uniform pressure shape are given in table 2 for several values of B^2 and N_θ/N_φ, and a typical set of these shapes is shown in figure 4. The calculation procedure was similar to that for the Newtonian flow shape except that $\sin \varphi$ was determined from

equation (28). For $N_\theta/N_\varphi = 0$ equations (29) and (30) could also be used to check the accuracy of the numerical procedure. Figure 4 shows that if $B^2 < 1$ and $N_\theta/N_\varphi = 0$, the curves intersect the $r = 0$ axis. Otherwise, they have been terminated at a nonzero value of r where $\sin \varphi = 1$; this result is similar to the result for the Newtonian pressure distribution with $N_\theta/N_\varphi > 0$. A typical comparison of the uniform pressure shape with the Newtonian flow shape for configurations with the same end points is shown in figure 5. The geometric differences are not large, an indication that the shape is not sensitive to the pressure distribution.

Catenary Shape

One disadvantage of the results obtained so far is that the coordinates of the meridian curve cannot be given in terms of elementary functions. The form of equation (20) suggests a somewhat simpler expression. If ρ^2 is replaced by ρ, equation (20) becomes

$$\frac{dz}{dr} = -\sinh C^2(1 - \rho) \tag{34}$$

Integrating equation (34) gives

$$\frac{z}{r_b} = \frac{1}{C^2}\left[\cosh C^2(1 - \rho) - 1\right] \tag{35}$$

which is the equation of a catenary. A comparison of the catenary given by equation (35) with the Newtonian flow shape is shown in figure 6 for $N_\theta/N_\varphi = 0$ and $N_\theta/N_\varphi = 0.15$. The curves do not differ greatly, especially the catenary and the curve for $N_\theta/N_\varphi = 0.15$. The stresses resulting from a Newtonian pressure distribution acting on these configurations are given in figure 7. Inasmuch as the catenary is very similar to the curve for $N_\theta/N_\varphi = 0.15$, circumferential tension stresses would be expected, which indeed is the case. The circumferential stress resultant reaches a value $\frac{1}{2} N_\varphi$ at the base. These stresses would be of benefit in stabilizing the shell for other loading conditions. It should be noted that the circumferential stress N_θ is very sensitive to small changes in the shape in the vicinity of the base; this sensitivity might require special consideration in the vehicle design.

The stress resultants for the Newtonian shape were obtained from equation (7) and the definition of A^2 as

$$\frac{N_\varphi}{qr_b} = \frac{1}{A^2\rho(1-\alpha)} \tag{36}$$

or for $N_\theta/N_\varphi = 0$

$$\frac{N_\varphi}{qr_b} = \frac{1}{A^2\rho} \tag{37}$$

The stresses in the catenary are obtained by solving equations (1) and (2), and the result is

$$\frac{N_\varphi}{qr_b} = \frac{2}{C^2}\left[1 + \frac{\ln \cosh C^2(1 - \rho)}{\rho C^2 \tanh C^2(1 - \rho)}\right] \tag{38}$$

$$\frac{N_\theta}{N_\varphi} = \frac{1}{\dfrac{\sinh^2 C^2(1 - \rho)}{\ln \cosh C^2(1 - \rho)} + \dfrac{\sinh C^2(1 - \rho)\cosh C^2(1 - \rho)}{\rho C^2}} \tag{39}$$

Although the catenary does not result in a constant value of N_θ/N_φ, N_θ and N_φ are always tensile quantities, and thus, the catenary conforms to the tension shell concept. The simplicity of the expression for the meridian shape of the catenary may be of advantage in subsequent aerodynamic or structural analysis.

CONCLUDING REMARKS

An entry vehicle configuration has been developed that resists the aerodynamic loadings at zero angle of attack and has only tensile stresses over a major portion of the vehicle surface. The configuration would be especially suited for application to vehicles entering thin atmospheres where low values of the ballistic coefficient are required. The use of a tension structure eliminates buckling as a design criteria, which can result in a significant increase in payload for these low values of ballistic coefficient. Calculated drag coefficients for the more promising configurations are relatively high (on the order of 1.5), which is desirable for a ballistic entry vehicle. A configuration can be determined for any ratio of circumferential stress to meridional stress, although practical limitations on overall dimensions may limit this ratio to approximately 0.3. The coordinates of the derived shapes cannot be expressed by elementary functions, but a catenary can be used to closely approximate the shape for purposes of analysis.

Langley Research Center,
National Aeronautics and Space Administration,
Langley Station, Hampton, Va., December 10, 1964.

REFERENCES

1. Anderson, Roger A.: Structures Technology - 1964. Astronaut. & Aeron., vol. 2, no. 12, Dec. 1964, pp. 14-20.

2. Roberts, Leonard: Entry Into Planetary Atmospheres. Astronaut. & Aeron., vol. 2, no. 10, Oct. 1964, pp. 22-29.

3. Flügge, Wilhelm: Stresses in Shells. Second printing, Springer-Verlag (Berlin), 1962, pp. 18-23.

4. Ince, E. L.: Ordinary Differential Equations. Dover Publ., Inc., 1956, pp. 23-25.

5. Jahnke; Emde; and Lösch: Tables of Higher Functions. Sixth ed., McGraw-Hill Book Co., Inc., 1960.

6. Houtz, N. E.: Optimization of Inflatable Drag Devices by Isotensoid Design. [Preprint] No. 64-437, Am. Inst. Aeron. Astronaut., June 29-July 2, 1964.

TABLE 1.- COORDINATES FOR NEWTONIAN FLOW SHAPE

r/r_b \ A^2	z/r_b for $N_\theta/N_\varphi = 0$						z/r_b for $N_\theta/N_\varphi = 0.1$					
	0.5	0.8	1.0	1.2	1.4	1.6	0.5	0.8	1.0	1.2	1.4	1.6
0	0.3430	0.5734	0.7460	0.9390	1.1597	1.4128						
.05	.3169	.5290	.6873	.8642	1.0646	1.2942	0.3642	0.6422	0.9216			
.10	.2910	.4849	.6290	.7893	.9702	1.1766	.3278	.5671	.7740	1.1009		
.15	.2654	.4414	.5715	.7156	.8774	1.0610	.2945	.5036	.6749	.8993	1.3444	
.20	.2402	.3986	.5151	.6434	.7866	.9485	.2633	.4463	.5913	.7692	1.0141	
.25	.2156	.3569	.4601	.5733	.6989	.8398	.2338	.3935	.5169	.6625	.8457	1.1104
.30	.1917	.3164	.4071	.5058	.6148	.7358	.2060	.3445	.4493	.5698	.7140	.8984
.35	.1686	.2775	.3562	.4412	.5343	.6372	.1797	.2988	.3874	.4871	.6026	.7417
.40	.1464	.2404	.3077	.3800	.4586	.5445	.1549	.2563	.3306	.4127	.5055	.6131
.45	.1254	.2052	.2620	.3225	.3878	.4587	.1317	.2169	.2785	.3455	.4198	.5036
.50	.1055	.1722	.2193	.2692	.3223	.3796	.1102	.1807	.2310	.2850	.3438	.4088
.55	.0870	.1416	.1798	.2200	.2625	.3078	.0904	.1475	.1879	.2307	.2766	.3265
.60	.0700	.1136	.1438	.1754	.2085	.2434	.0723	.1176	.1492	.1824	.2175	.2550
.65	.0545	.0882	.1114	.1355	.1605	.1866	.0560	.0908	.1149	.1399	.1660	.1935
.70	.0407	.0658	.0829	.1005	.1185	.1373	.0417	.0673	.0849	.1030	.1218	.1413
.75	.0288	.0463	.0583	.0704	.0829	.0956	.0293	.0472	.0594	.0718	.0846	.0977
.80	.0187	.0301	.0378	.0455	.0534	.0615	.0190	.0305	.0383	.0462	.0543	.0625
.85	.0107	.0172	.0215	.0259	.0303	.0348	.0108	.0174	.0218	.0262	.0307	.0352
.90	.0048	.0077	.0097	.0117	.0136	.0156	.0049	.0078	.0098	.0117	.0137	.0157
.95	.0012	.0020	.0025	.0030	.0034	.0039	.0012	.0020	.0025	.0030	.0035	.0040
1.00	0	0	0	0	0	0	0	0	0	0	0	0

r/r_b \ A^2	z/r_b for $N_\theta/N_\varphi = 0.3$						z/r_b for $N_\theta/N_\varphi = 0.5$					
	0.5	0.8	1.0	1.2	1.4	1.6	0.5	0.8	1.0	1.2	1.4	1.6
0												
.05												
.10	0.4470											
.15	.3771											
.20	.3241	0.6271					0.4348					
.25	.2795	.5067	0.8086				.3482					
.30	.2405	.4220	.5927				.2874					
.35	.2056	.3534	.4781	0.6570			.2387	0.4441				
.40	.1743	.2950	.3909	.5107	0.6881		.1978	.3499	0.5015			
.45	.1460	.2443	.3192	.4068	.5164	0.6761	.1627	.2796	.3787	0.5249		
.50	.1205	.1997	.2584	.3242	.4008	.4951	.1322	.2229	.2940	.3816	0.5070	
.55	.0976	.1606	.2061	.2558	.3111	.3747	.1057	.1757	.2280	.2879	.3602	0.4565
.60	.0772	.1262	.1610	.1981	.2383	.2827	.0826	.1359	.1745	.2168	.2644	.3199
.65	.0592	.0963	.1222	.1494	.1783	.2092	.0627	.1024	.1304	.1603	.1926	.2282
.70	.0436	.0707	.0893	.1086	.1287	.1499	.0457	.0742	.0940	.1146	.1364	.1596
.75	.0304	.0491	.0618	.0748	.0883	.1022	.0316	.0510	.0643	.0780	.0922	.1070
.80	.0196	.0314	.0395	.0471	.0560	.0645	.0201	.0324	.0407	.0492	.0578	.0667
.85	.0111	.0177	.0222	.0268	.0313	.0360	.0113	.0181	.0227	.0274	.0321	.0368
.90	.0049	.0079	.0099	.0119	.0139	.0159	.0050	.0080	.0100	.0121	.0141	.0162
.95	.0012	.0020	.0025	.0030	.0035	.0040	.0012	.0020	.0025	.0030	.0035	.0040
1.00	0	0	0	0	0	0	0	0	0	0	0	0

TABLE 2.- COORDINATES FOR UNIFORM PRESSURE SHAPE

	z/r_b for $N_\theta/N_\varphi = 0$						z/r_b for $N_\theta/N_\varphi = 0.1$					
r/r_b \ B^2	0.5	0.8	1.0	1.2	1.4	1.6	0.5	0.8	1.0	1.2	1.4	1.6
0	0.3672	0.7393	∞									
.05	.3384	.6728	1.8156				0.3970					
.10	.3097	.6072	1.3283				.3548	0.9410				
.15	.2815	.5433	1.0451				.3166	.7128				
.20	.2538	.4820	.8464				.2813	.5913				
.25	.2268	.4236	.6947				.2483	.4975				
.30	.2008	.3687	.5732				.2173	.4195				
.35	.1758	.3175	.4730				.1884	.3526	0.6071			
.40	.1520	.2701	.3888				.1615	.2943	.4528			
.45	.1295	.2267	.3173	0.4906			.1366	.2433	.3529			
.50	.1085	.1873	.2560	.3623			.1136	.1985	.2769	0.4284		
.55	.0891	.1517	.2034	.2738	0.4187		.0927	.1591	.2160	.3001		
.60	.0713	.1200	.1583	.2061	.2764		.0738	.1248	.1658	.2190	0.3082	
.65	.0554	.0921	.1199	.1524	.1937	0.2572	.0570	.0951	.1243	.1591	.2052	0.2882
.70	.0412	.0679	.0874	.1092	.1346	.1664	.0422	.0697	.0899	.1126	.1397	.1747
.75	.0290	.0474	.0605	.0745	.0900	.1077	.0296	.0484	.0618	.0762	.0923	.1108
.80	.0188	.0305	.0387	.0472	.0562	.0659	.0191	.0310	.0393	.0480	.0572	.0672
.85	.0107	.0173	.0218	.0264	.0312	.0361	.0109	.0175	.0221	.0267	.0315	.0366
.90	.0048	.0078	.0098	.0118	.0138	.0158	.0049	.0078	.0098	.0118	.0139	.0160
.95	.0012	.0020	.0025	.0030	.0035	.0040	.0012	.0020	.0025	.0030	.0035	.0040
1.00	0	0	0	0	0	0	0	0	0	0	0	0

	z/r_b for $N_\theta/N_\varphi = 0.3$						z/r_b for $N_\theta/N_\varphi = 0.5$					
r/r_b \ B^2	0.5	0.8	1.0	1.2	1.4	1.6	0.5	0.8	1.0	1.2	1.4	1.6
0												
.05												
.10	0.5651											
.15	.4336											
.20	.3618											
.25	.3061						0.4227					
.30	.2595						.3261					
.35	.2193	0.4920					.2623					
.40	.1840	.3678					.2129					
.45	.1527	.2874					.1724	0.3720				
.50	.1251	.2259	0.3422				.1384	.2653				
.55	.1006	.1763	.2483	0.4430			.1095	.1981	0.3039			
.60	.0791	.1355	.1834	.2542			.0849	.1480	.2065	0.3363		
.65	.0603	.1015	.1340	.1748	0.2372		.0640	.1087	.1455	.1957	0.3254	
.70	.0442	.0734	.0952	.1203	.1514	0.1963	.0464	.0774	.1010	.1291	.1663	0.2351
.75	.0307	.0504	.0695	.0799	.0973	.1179	.0319	.0525	.0674	.0839	.1029	.1263
.80	.0197	.0320	.0406	.0496	.0593	.0698	.0203	.0330	.0419	.0513	.0615	.0727
.85	.0111	.0179	.0226	.0273	.0323	.0375	.0113	.0183	.0231	.0280	.0331	.0384
.90	.0049	.0079	.0100	.0120	.0141	.0162	.0050	.0081	.0101	.0122	.0143	.0164
.95	.0012	.0020	.0025	.0030	.0035	.0040	.0013	.0020	.0025	.0030	.0035	.0040
1.00	0	0	0	0	0	0	0	0	0	0	0	0

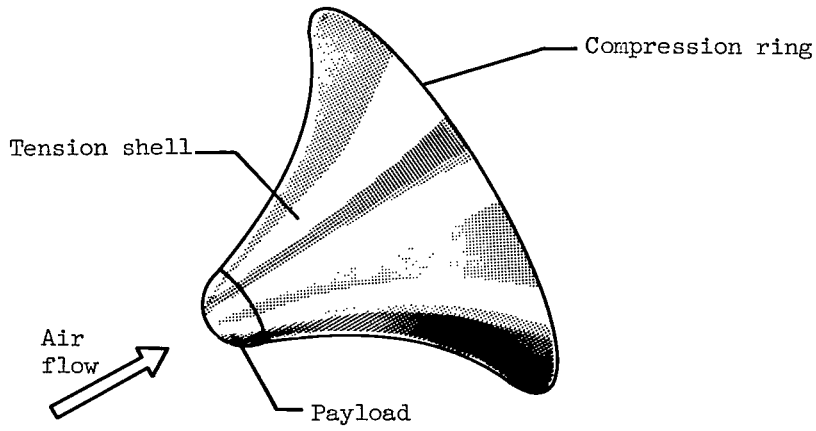

(a) Schematic diagram.

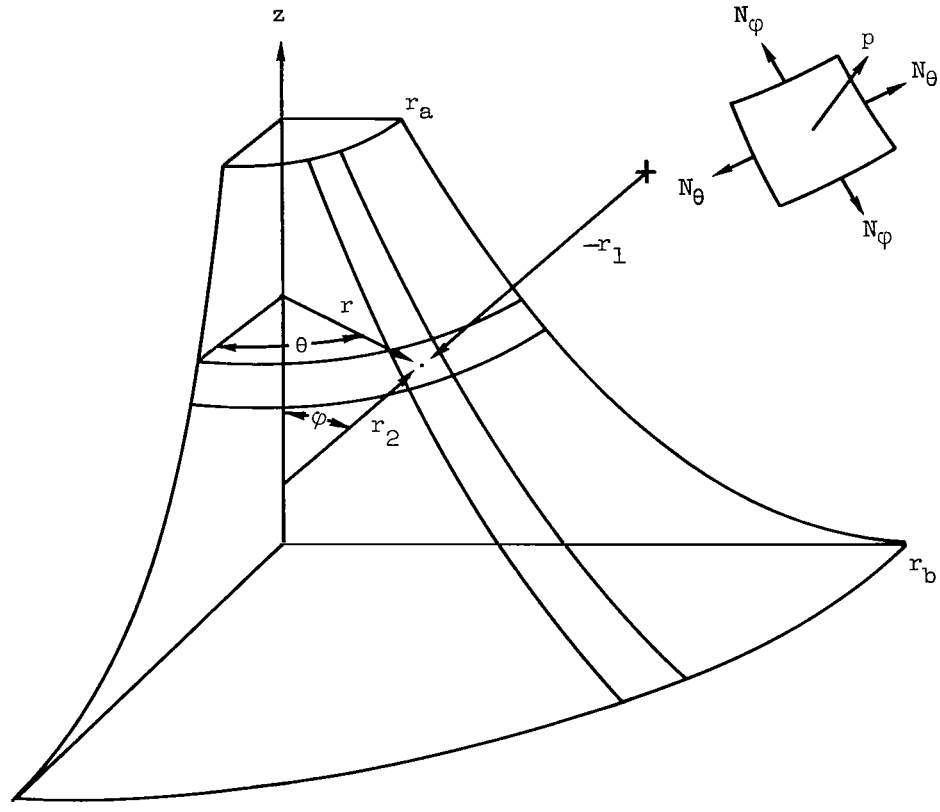

(b) Configuration and coordinate system.

Figure 1.- Tension shell entry vehicle.

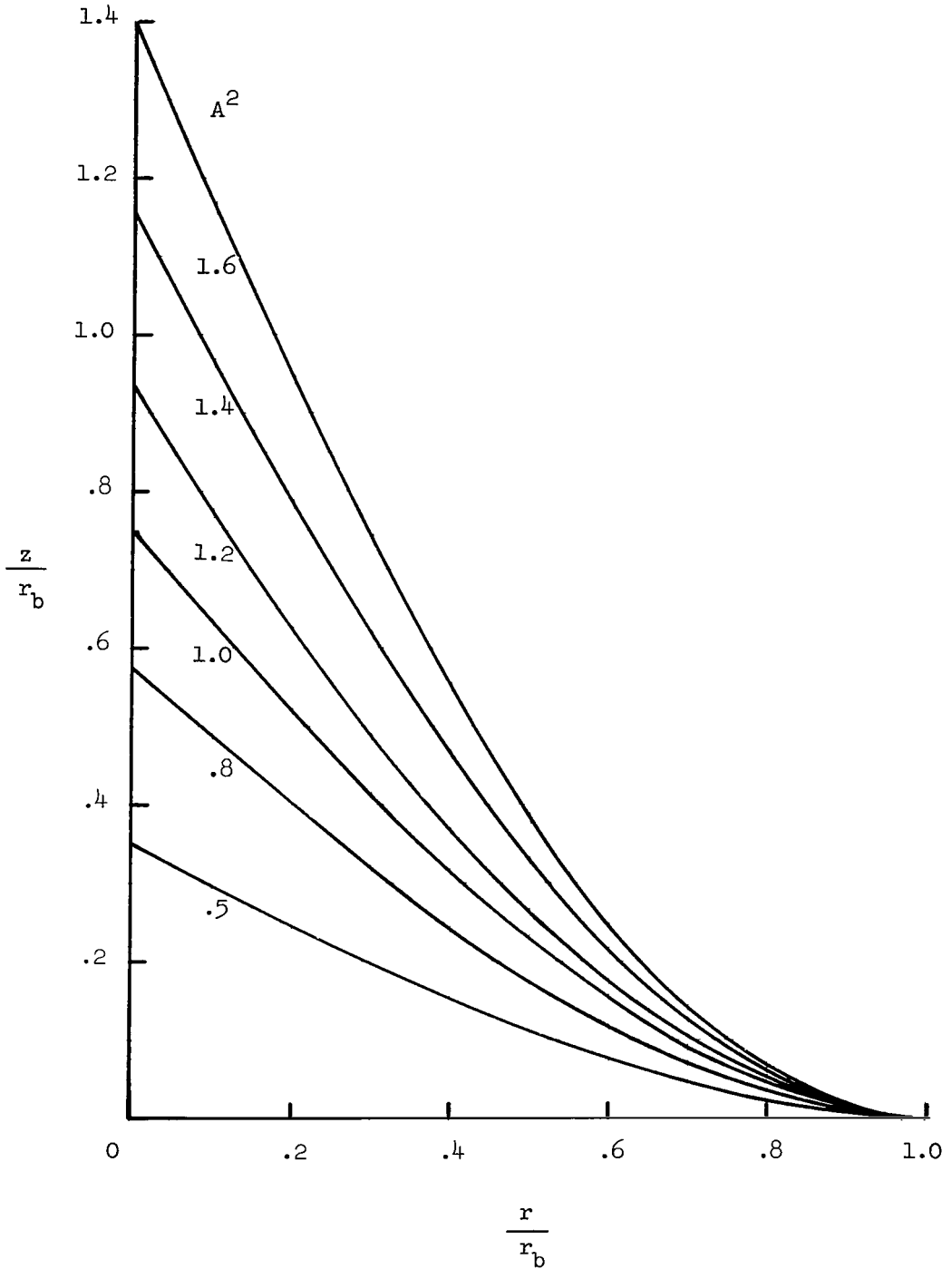

(a) Variation with shape parameter A^2. $N_\theta/N_\varphi = \alpha = 0$.

Figure 2.- Newtonian flow shape.

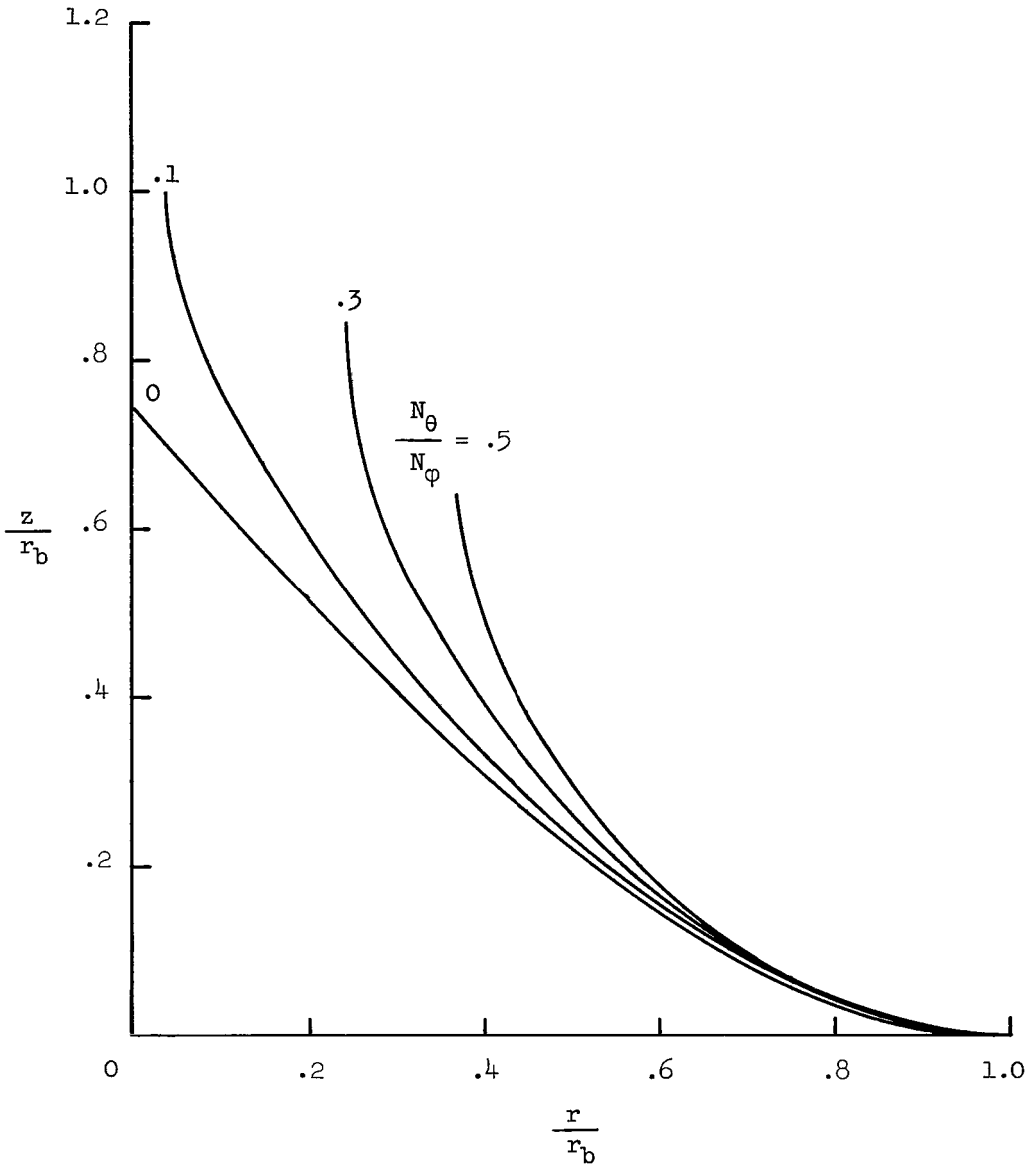

(b) Variation with stress ratio N_θ/N_φ. $A^2 = 1$.

Figure 2.- Concluded.

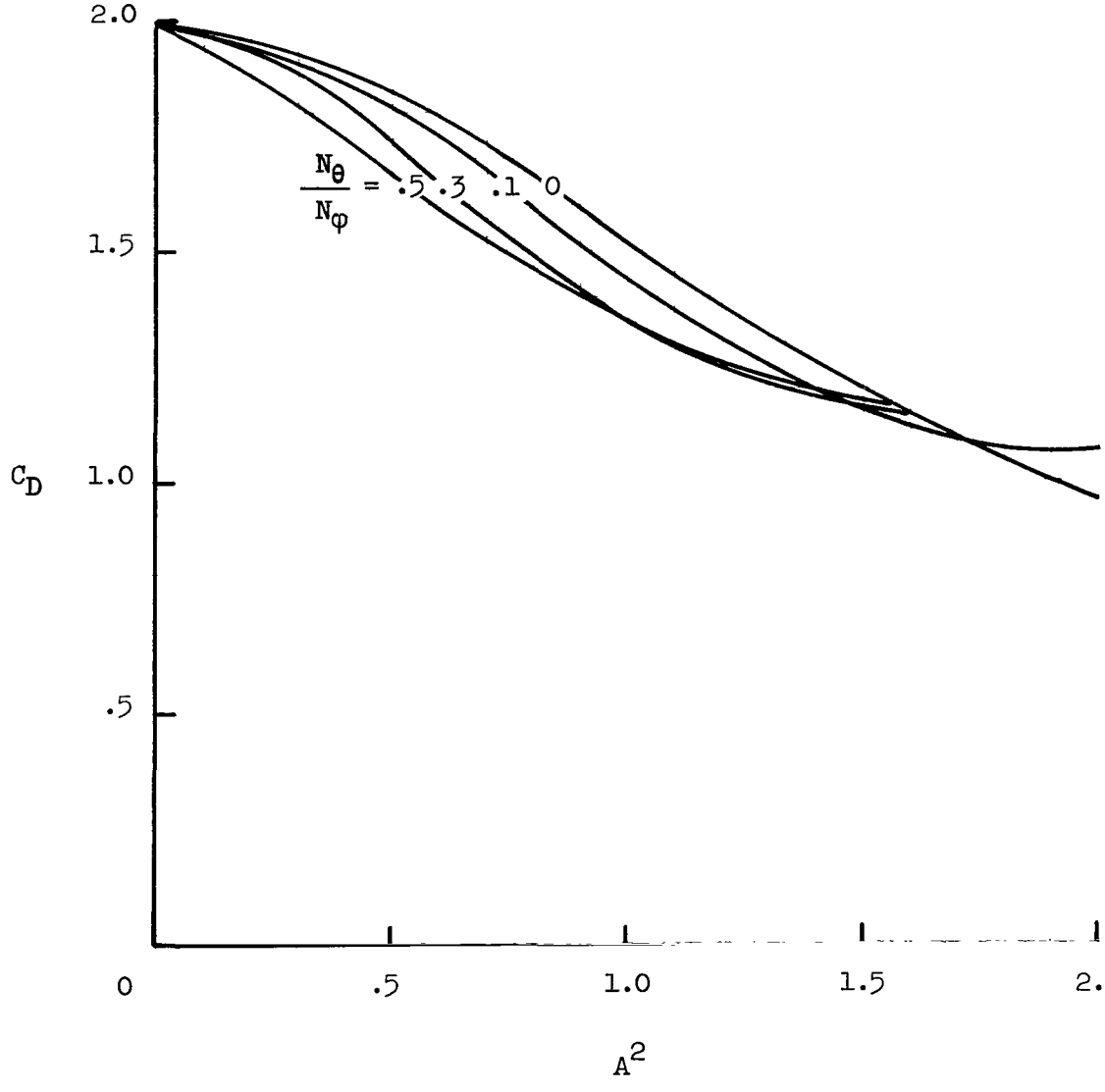

Figure 3.- Variation of drag coefficient with shape parameter A^2 for various values of N_θ/N_φ.

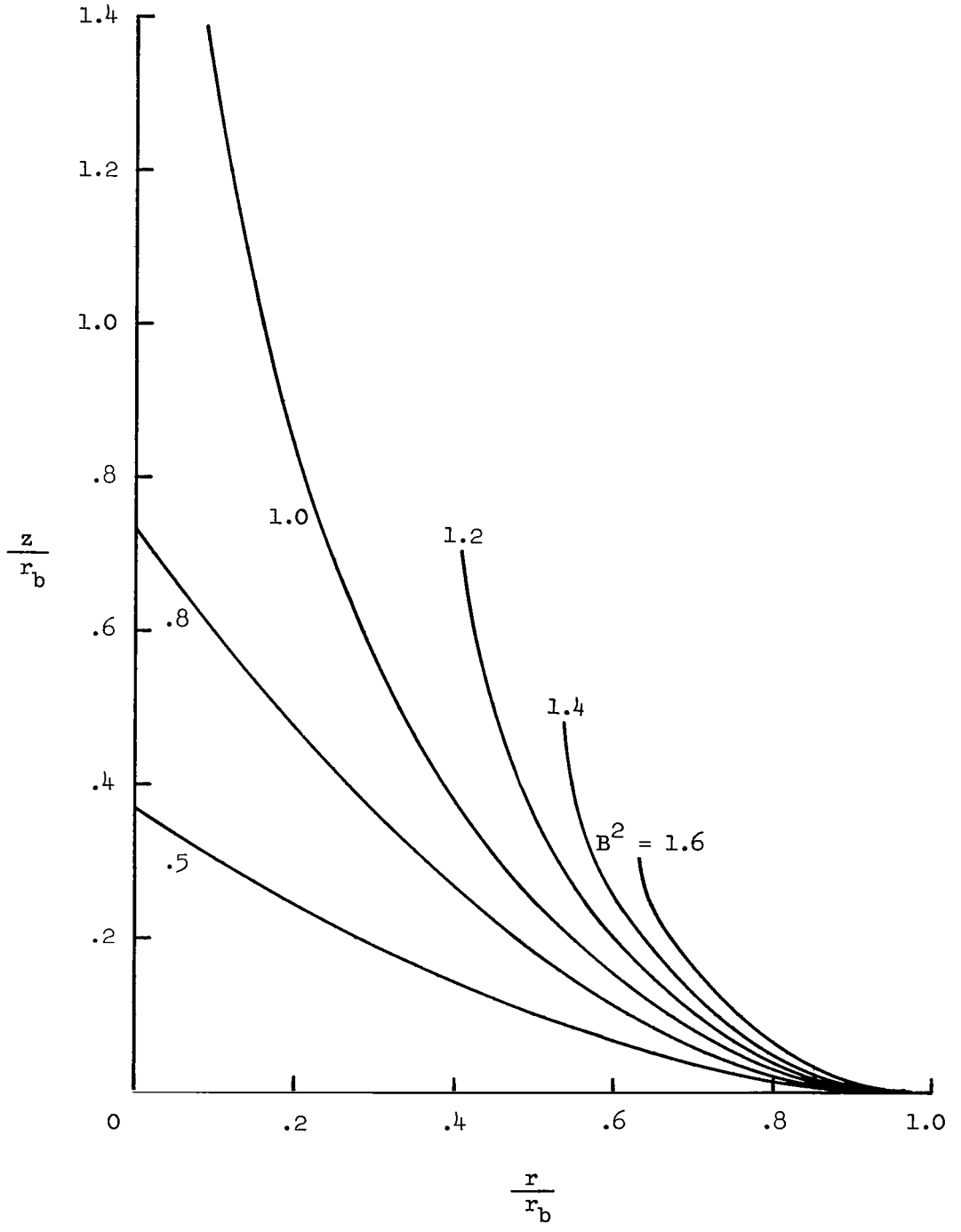

(a) Variation with B^2. $N_\theta/N_\varphi = 0$.

Figure 4.- Uniform pressure shape.

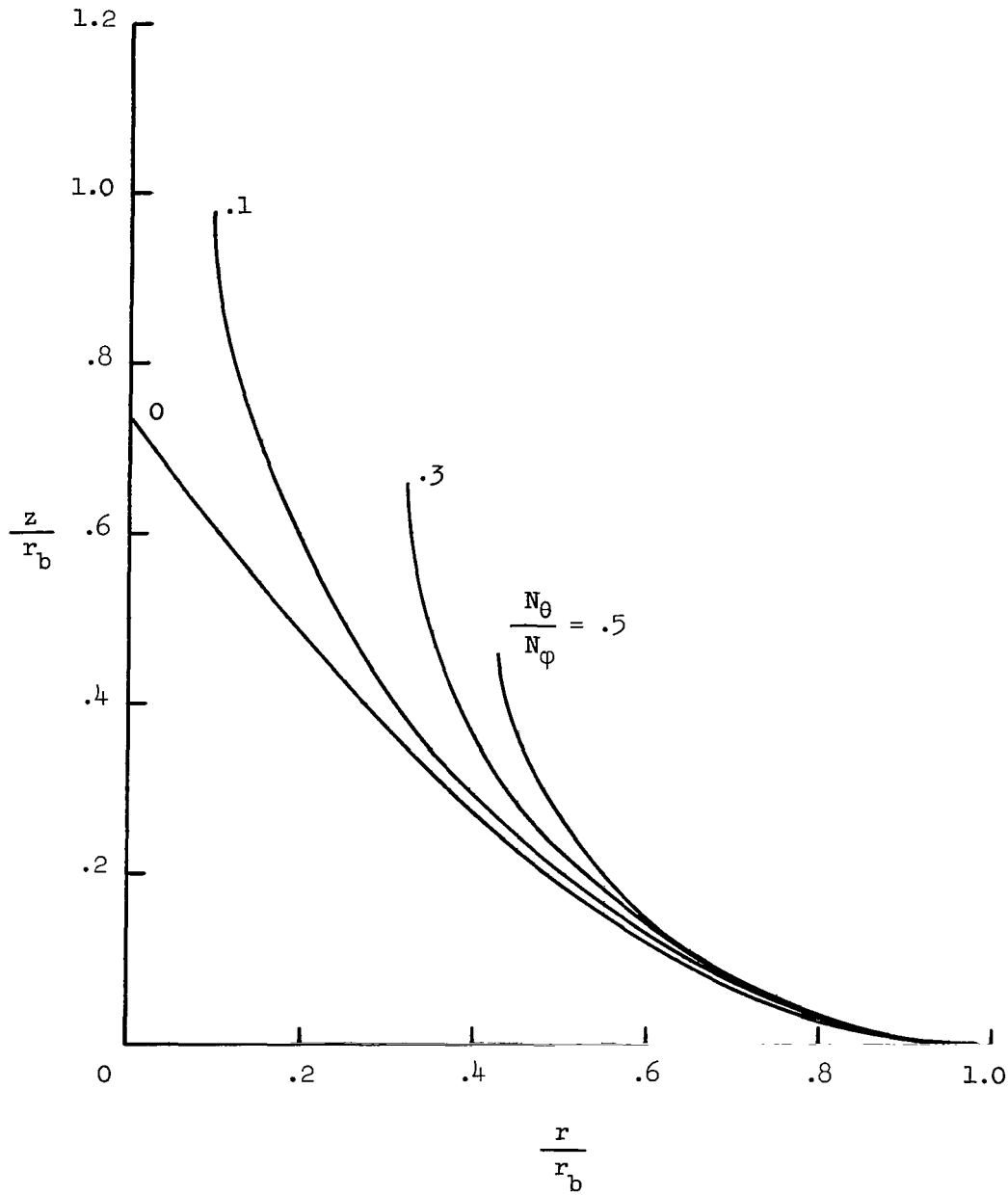

(b) Variation with N_θ/N_φ. $B^2 = 0.8$.

Figure 4.- Concluded.

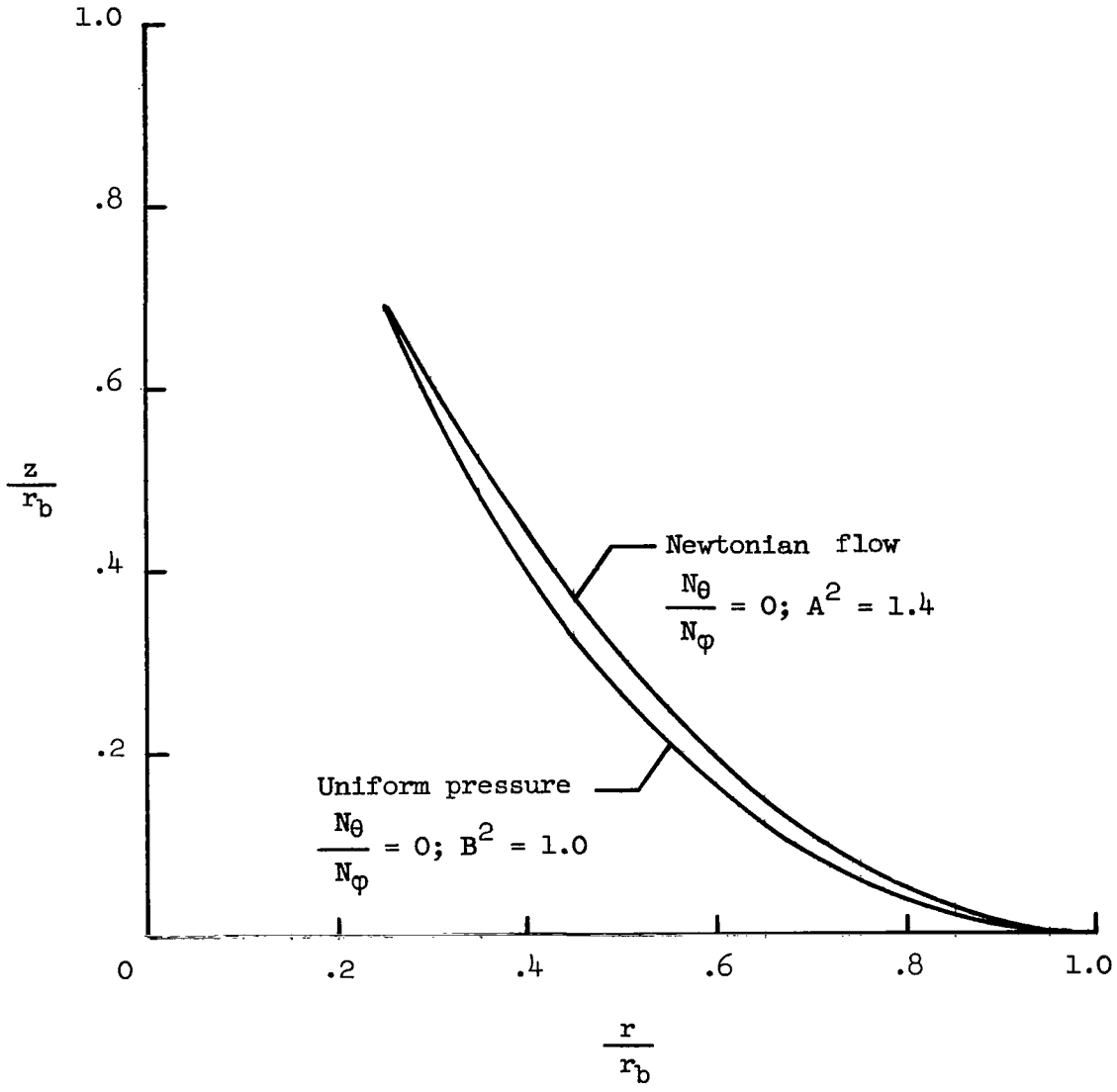

Figure 5.- Effect of pressure distribution on shape of tension shell.

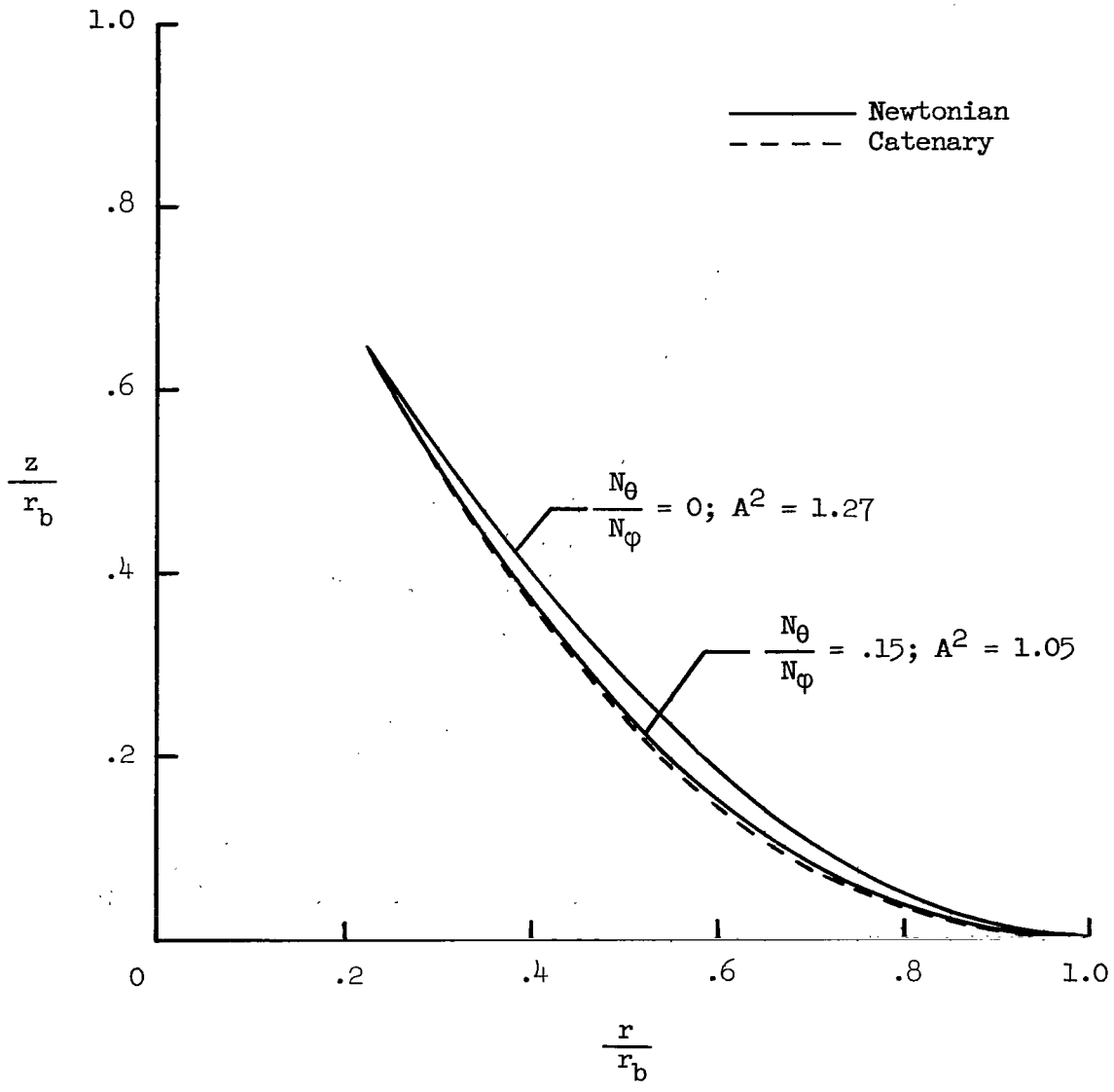

Figure 6.- Comparison of Newtonian flow shape with catenary shape.

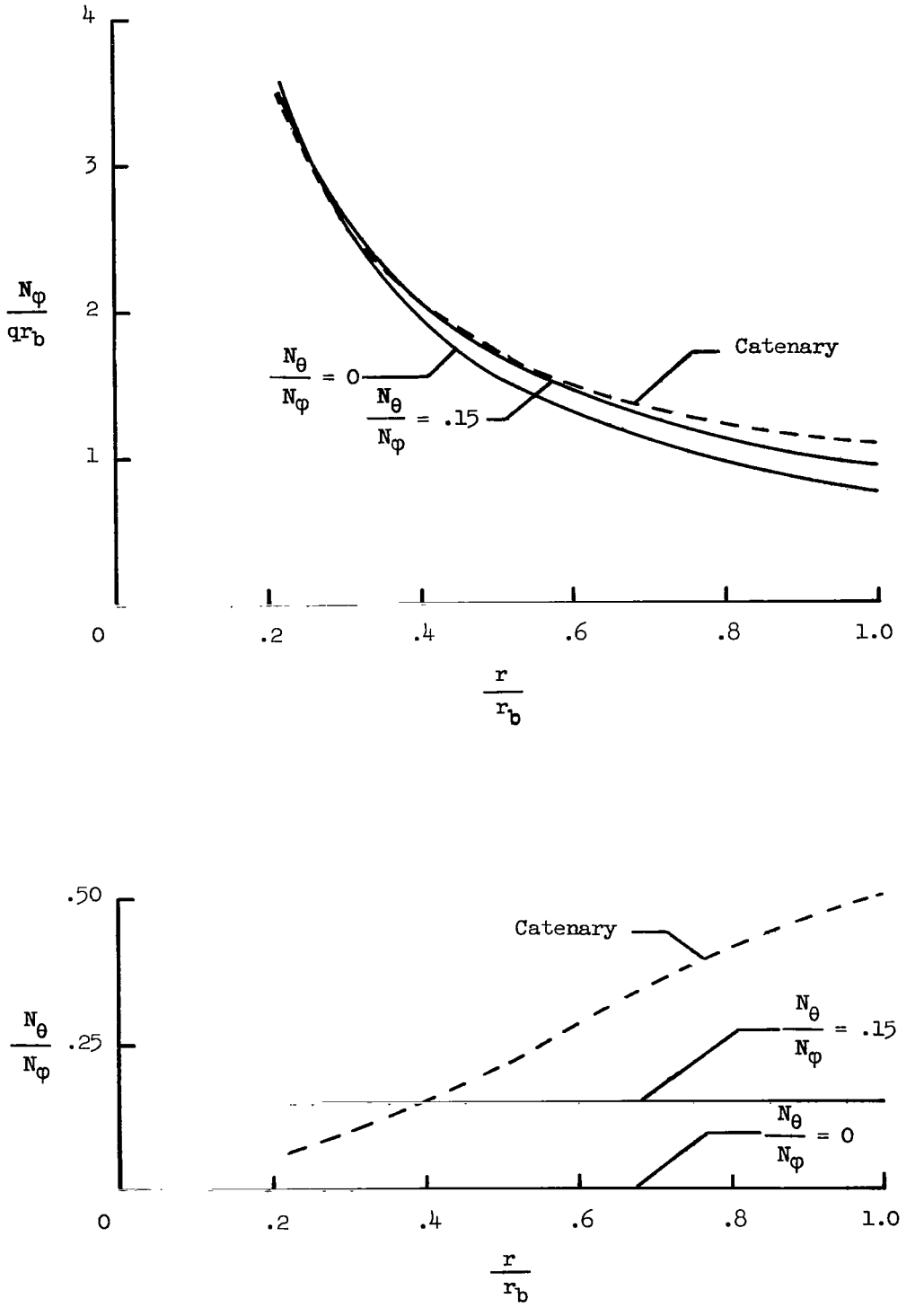

Figure 7.- Stress resultants for Newtonian flow shape and catenary shape.

2/22/85

"The aeronautical and space activities of the United States shall be conducted so as to contribute . . . to the expansion of human knowledge of phenomena in the atmosphere and space. The Administration shall provide for the widest practicable and appropriate dissemination of information concerning its activities and the results thereof."

—NATIONAL AERONAUTICS AND SPACE ACT OF 1958

NASA SCIENTIFIC AND TECHNICAL PUBLICATIONS

TECHNICAL REPORTS: Scientific and technical information considered important, complete, and a lasting contribution to existing knowledge.

TECHNICAL NOTES: Information less broad in scope but nevertheless of importance as a contribution to existing knowledge.

TECHNICAL MEMORANDUMS: Information receiving limited distribution because of preliminary data, security classification, or other reasons.

CONTRACTOR REPORTS: Technical information generated in connection with a NASA contract or grant and released under NASA auspices.

TECHNICAL TRANSLATIONS: Information published in a foreign language considered to merit NASA distribution in English.

TECHNICAL REPRINTS: Information derived from NASA activities and initially published in the form of journal articles.

SPECIAL PUBLICATIONS: Information derived from or of value to NASA activities but not necessarily reporting the results of individual NASA-programmed scientific efforts. Publications include conference proceedings, monographs, data compilations, handbooks, sourcebooks, and special bibliographies.

Details on the availability of these publications may be obtained from:

SCIENTIFIC AND TECHNICAL INFORMATION DIVISION

NATIONAL AERONAUTICS AND SPACE ADMINISTRATION

Washington, D.C. 20546